Reviews in Mineralogy & Geochemistry
Vol. 58, pp. 499-525, 2005

Thermochronometers in Sedimentary Basins

Phillip A. Armstrong

Dept. of Geological Sciences
California State University, Fullerton
800 N. State College Blvd.
Fullerton, CA 92831
parmstrong@fullerton.edu

INTRODUCTION

Sedimentary basins, both modern and ancient, cover most of Earth's land and subsea surface, and provide some of the best natural laboratories for studying and constraining geologic processes. The record of sedimentation, burial, erosion, and uplift provides a rich history that can be combined with various analytical and modeling techniques to evaluate: (1) processes that lead to basin formation; (2) deformation of regions related to plate tectonic effects; (3) timing and duration of hydrocarbon generation, migration, and trapping; (4) past and present effects of fluid flow in basin deposits; and (5) past climate change. Sedimentary basins have been classified by many workers (e.g., Bally and Snelson 1980; Dickinson 1993; Ingersoll and Busby 1995). Ingersoll and Busby (1995) generally classify the basins as forming in divergent settings, intraplate regions, convergent settings, transform settings, and hybrid settings. Many mechanisms have been proposed for the formation of the different styles of basins including, but not limited to, crustal thinning, sedimentary and tectonic loading, subcrustal loading, and mantle lithospheric thickening (e.g., Ingersoll and Busby 1995).

Thermochronometers have played an increasingly important role in the evaluation of both intra- and interbasin processes. Thermochronometers, especially the lower-temperature apatite fission-track and apatite (U-Th)/He dating, are now commonly combined with burial and thermal history analysis and modeling to provide important constraints on the timing and duration of heating/cooling events that can be used to evaluate hydrocarbon systems as well as structural and basin-forming mechanisms.

Past reviews of thermochronometer use in sedimentary basins are given by Naeser et al. (1989), Green et al. (1989a), Naeser (1993), and Giles and Indrelid (1998). Rather than review each study of thermochronometer use in sedimentary basins during the last decade, in this chapter some of the fundamental concepts used to evaluate the present-day thermal field for sedimentary basins, how a basin analyst would evaluate and combine burial and thermal histories, and the main thermochronometers used in sedimentary basin analysis are summarized. Finally, several recent case studies that illustrate the modern uses of thermochronometers in sedimentary basins are reviewed.

PROCESSES THAT AFFECT BASIN TEMPERATURES – THE HEAT BUDGET

Present-day temperatures and paleotemperatures help constrain models of processes that occur within and below sedimentary basins. These temperatures, and their thermochronologic signatures, are the net result of several different thermal and tectonic processes taking place at different spatial and temporal scales. Armstrong and Chapman (1998) broadly group these

1529-6466/05/0058-0019$05.00 DOI: 10.2138/rmg.2005.58.19

processes into six categories: (1) variations in basal heat flow that might be due to lateral temperature changes in the mantle; (2) vertical and/or lateral changes in rock properties such as heat production or thermal conductivity within or below the basin; (3) heat-flow perturbations resulting from exhumation or burial; (4) thermal effects of fluid flow; (5) anomalous heat flow related to magmatic processes such as intrusion emplacement; and (6) tectonic heating or cooling caused by lithospheric thinning and thickening.

Any combination of these processes can perturb the thermal field of a sedimentary basin at any point in its history. Standard basin analysis techniques (e.g., Allen and Allen 1990) make quantifying the thermal effects of some of these processes possible (i.e., exhumation and burial), thus making interpretations of other processes possible if indicators that constrain past temperatures are available.

PRESENT-DAY THERMAL FIELD

Any thermal history modeling exercise in a sedimentary basin must honor the present-day temperature constraints for that basin. Among the principal locations for making the temperature measurements are oil and gas exploration wells. Uncorrected bottom-hole temperatures (BHT) are measured as part of the routine geophysical well logging and typically range from 25–175 °C at depths of 1–5 km. These BHTs must then be corrected for the thermal disturbance caused by drilling and well circulation. There are several reviews of methods for correcting BHTs (e.g., Deming 1989; Funnell et al. 1996), but the method generally includes extrapolating temperatures to infinite time based on multiple temperature measurements at different times following the stoppage of drilling at a particular depth.

The temperature profile between discrete BHTs is computed and depends on rock thermophysical properties such as thermal conductivity and heat production. Thermal conductivity data can be measured in the lab on available drill core or drill cuttings, however, these values relate to discrete sections of the well and specific rock types. One strategy is to establish end-member thermal conductivity values for the different rock types present in a particular basin, then apply these values to similar rock types within the basin based on well log data. For example, Funnell et al. (1996) measured sandstone and shale thermal conductivities of 4.0 and 2.7 $Wm^{-1}K^{-1}$, respectively, for the Taranaki Basin in New Zealand. Heat production within the sedimentary column itself is typically small and often a neglected contributor to the basin's overall heat budget. Typical specific heat production (mass specific) values are ~10–100 × 10^{-5} μW/kg for different sedimentary rock types; this heat production amounts to a heat flow increase of ~1 mW/m^2 for every 1 km of sedimentary section in the basin. All thermal conductivity and specific heat production estimates must be corrected for porosity prior to using them in subsurface temperature and heat flow computations (see below). Porosity is often considered to decrease exponentially with depth (e.g., Magara 1976; Funnell et al. 1996) in sedimentary basins, though many other models have been proposed (e.g., Issler 1992).

Once thermophysical properties of the section are determined and corrected, variations in temperature between discrete BHTs can be computed. The temperature as a function of depth for steady-state heat conduction in a horizontally layered sedimentary section is given by:

$$T(z) = T_0 + \sum_{i=1}^{n}\left[\frac{q_{i-1}\cdot\Delta z_i}{\lambda_i} - \frac{A_i\Delta z_i^{\,2}}{2\lambda_i}\right] \tag{1}$$

where

$$q_i = q_{i-1} - A_i\Delta z_i \tag{2}$$

and T_0 is the surface temperature, λ_i, Δz_i, and A_i are thermal conductivity, thickness, and volumetric heat production, respectively, for the i^{th} depth interval. q_{i-1} is the heat flow at the top of the i^{th} interval and q_0 is the surface heat flow. The temperature-depth profile can then be determined by iterating on the surface heat flow until the difference between BHTs and model temperatures at those depths is minimized (Funnell et al. 1996).

BUILDING A BURIAL AND THERMAL HISTORY

Because sedimentary basins retain a record of burial and exhumation, it is possible to build a burial history and couple that to a thermal history based on the physics of heat transport. Hermanrud (1993), Lerche (1993), and Poelchau et al. (1997) provide reviews on the concepts of basin simulation. The basin analyst generally is concerned with burial, erosion, thermal history, hydrocarbon generation, expulsion, and migration, trap formation, fluid accumulations, and overpressuring. We restrict our discussion to the burial, erosion, and thermal history aspects because they are the parts primarily constrained by thermochronometry. A general overview is given below, and the basic scheme of implementation is shown in Figure 1.

Input parameters for the burial/erosion history include known stratigraphic thicknesses and ages, age bounds on erosional unconformities, and porosity-depth relations. The thickness of each stratigraphic unit is decompacted based on the present-day thickness and an assumed porosity-depth relation (e.g., Schlater and Christie 1980). Input sedimentation rates then are estimated from the thicknesses of the decompacted sediments and their ages. Once timing and rates of burial, and erosion, are determined for each stratigraphic unit, the units can be redeposited or eroded sequentially to construct the burial history. At each time step, material properties are adjusted for depth changes and the temperatures are computed, usually based

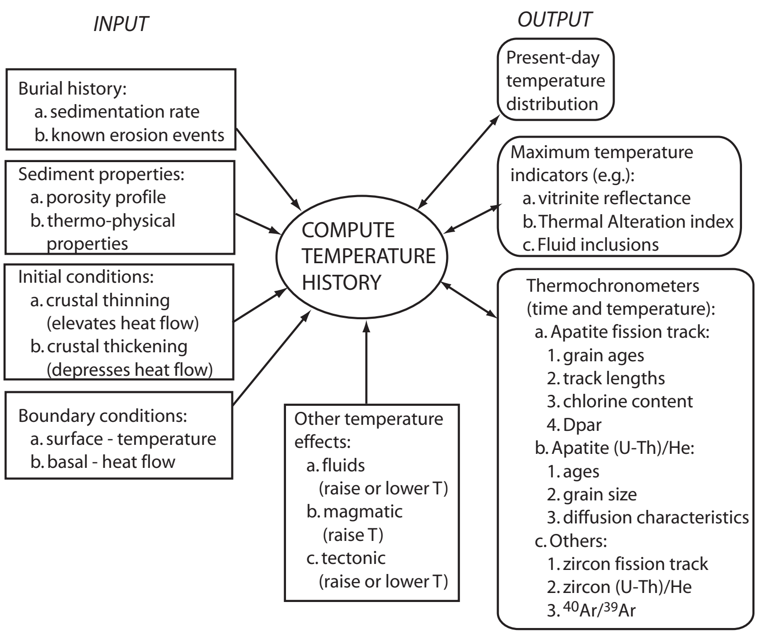

Figure 1. General schematic showing the basic input and output information used to combine burial and thermal histories with thermochronometer data.

on transient conductive heat flow laws. At the end of the simulation, model temperatures and thermochronologic information are compared with measured values and the model is iterated until good fits are obtained. Poor fits to these data sets can then be evaluated and remodeled by incorporating more complex histories that include alternative temperature effects such as those caused by intrusion emplacement, fluid flow, and/or tectonic perturbations (i.e., crustal thinning or thickening; Armstrong and Chapman 1998).

Most of the coupled burial-thermal history simulators assume one-dimensional conductive heat flow. However, large potential temperature variations in sedimentary basins can be caused by lateral thermal conductivity variations and fault-related heat advection. In such cases, heat will be partially refracted across thermal conductivity boundaries such as faults and into high-conductivity regions, which causes temperature to increase in the high-conductivity regions and decrease in the low-conductivity regions. Weir and Furlong (1987) demonstrated that 2D simulations are necessary to account for the heat refraction problem when the width to depth ratio of a basin is less than approximately 5 to 1. Therefore, except for very narrow and deep basins, a 1D solution for these types of burial histories is generally good enough, especially given the uncertainties in sedimentation rates, erosion rates, and thermochronologic modeling.

The boundary conditions used in most thermal modeling routines include an upper surface temperature boundary and a lower heat flow boundary. Mean annual surface temperatures generally are estimated from known environmental conditions at the time of burial (paleoclimate, paleogeography, paleobathymetry). These temperatures can vary substantially and propagate rapidly into the basin sediments. In the Taranaki Basin, surface temperatures based on marine fauna, land flora, and oxygen isotopic data indicate surface temperature changes of ~15 °C in the late Cenozoic (Armstrong et al. 1996), which can affect apatite fission-track ages in the subsurface (e.g., O'Sullivan and Brown 1998). The lower heat flow boundary condition should be placed at sufficient depth to allow the lithosphere to be affected by near surface transient affects. It is unrealistic to place the lower boundary condition at the base of the sediments in the basin because that would imply that the sediments are decoupled thermally from the basement rocks below. Nielsen and Balling (1990) showed that excluding transient thermal coupling between basin strata and the underlying basement can lead to inaccurate estimates of heat flow and temperature structure of a basin. The lower heat flow boundary should be placed at depths of 10's of kilometers. In many models, it is the heat flow at the bottom boundary that is adjusted during the burial–thermal history simulation to account for the temperatures at the end of the simulation (Armstrong and Chapman 1998).

All thermal history simulations must begin with an assumed set of initial conditions. Normally the initial condition is based on presumed heat flow conditions at the time of initial basin formation. For example, rift-related basins will include initially high heat flow related to thinning of the lithosphere (e.g., McKenzie 1978) where the stretching factor is computed from analysis of tectonic subsidence. Alternatively, initial heat flow might be lower than present-day in cases where basins form in response to crustal thickening at convergent plate margins. The transient effects of these lithospheric-scale processes can last for 10^7 years or more and should be included in thermal history analyses if possible. Thermal modeling programs generally allow the user to apply stretching factors with implicit heat flow variations or to apply explicit high or low heat flow during the simulations. Unfortunately, low-temperature thermochronometers are less sensitive to the early heat flow conditions than they are to maximum temperature and burial conditions that usually occur after the initial thermal conditions wane. Nielsen (1996) and Ferrero and Gallagher (2002) used stochastic thermal modeling to constrain heat flow changes through the basin history. These stochastic models utilize proposed burial histories, vitrinite reflectance, and present-day temperatures to place bounds on paleo heat flow values.

If input parameters such as burial history, sediment thermophysical properties, and initial conditions can be determined, or at least reasonably bracketed, then potential temperature histories can be computed for a basin. The suite of computed thermal histories and their output can then be compared to present-day temperature conditions, maximum temperature indicators such as vitrinite reflectance, and to computed thermal histories for the different thermochronometers (mainly apatite fission-track and apatite (U-Th)/He—see later sections) to determine if the temperature history from burial information is acceptable (Fig. 1). Unacceptable temperature histories might require additional thermal effects to explain the thermal data. Such effects might include fluid flow, which can raise or lower subsurface temperatures, or localized magmatic intrusion, which raises subsurface temperatures.

THERMOCHRONOMETERS USED IN SEDIMENTARY BASINS

Several thermochronometers can be used in the study of sedimentary basins, including apatite fission-track (AFT), zircon fission-track (ZFT), apatite and zircon (U-Th)/He dating, $^{40}Ar/^{39}Ar$ in white mica and potassium feldspar. These thermochronometers have different and sometimes overlapping closure temperatures ranging from ~70 to >200 °C. In this review, the lower-temperature thermochronometers of apatite fission-track and apatite (U-Th)/He are mainly illustrated. In the following sections, the dating methods as they pertain to sedimentary basins are outlined; details of the measurement techniques and general interpretations are given in earlier chapters of this volume.

Apatite fission-track dating

The fundamentals and theory of AFT thermochronology are discussed in this volume by Donelick et al. (2005) and Tagami et al. (2005) and by other recent reviews (e.g., Gleadow et al. (2002). Furthermore, the application of AFT thermochronology to sedimentary basins in particular has been outlined by several papers in the last couple decades (Gleadow et al. 1983; Green et al. 1989a; Naeser et al. 1989; Naeser 1993; Giles and Indrelid 1998).

AFT analysis is particularly important to basin analysis and hydrocarbon exploration because its range of annealing temperatures, which generally has been considered to be between 60 and 120 °C in most studies, approximately corresponds with liquid hydrocarbon generation temperatures at geologic time scales. However, this generally used annealing temperature range (60–120 °C) does not reflect the annealing range of apatite grains encountered in many samples, which has bounds of approximately 50–150 °C depending on apatite composition—see below and Donelick et al. (2005) in this volume; apatite kinetic data should be determined for all dated grains.

Naeser (1979) provides a good example of the expected effects of AFT age with temperature in a sedimentary basin succession that is currently at maximum temperature at any depth. Figure 2 shows that the shallowest/coolest samples should have relatively old AFT ages, primarily due to containing detrital AFT grain ages that are at least as old as the depositional age of the strata. The distribution of the detrital AFT grain ages within a single sample in the shallow section may show considerable scatter reflecting variations in apatite chemistry (see below), variations in source regions with different exhumation histories, or both. In the shallow-section, AFT sample ages can either increase or decrease down section. An increase in the shallow AFT sample ages down section usually reflects detrital input from progressively younger denuded source terrains within which the apatites had been partially or totally reset. Alternatively, a decrease in the shallow AFT sample ages down-section usually reflects sourcing from regions where the apatites were not reset.

Below the depth where temperature is ~50–70 °C (depending on composition), fission-track annealing begins and AFT ages start to decrease. For apatites with the same annealing

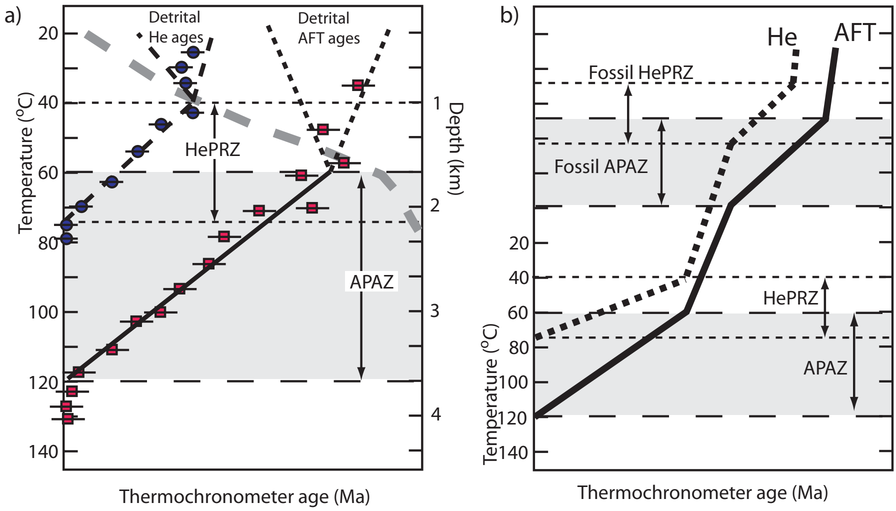

Figure 2. Idealized low-temperature thermochronometer versus temperature profiles in a well. Plot a) shows scenario where no uplift and exhumation has occurred. Apatite fission-track ages (filled squares) in this case are all older than apatite (U-Th)/He ages (filled circles). The thick dashed gray line is stratigraphic age. APAZ represents apatite partial annealing zone. HePRZ represents the apatite helium partial retention zone. In b), the sequence has been uplifted toward surface to give fossil APAZ and HePRZ (see text). Note that in b), temperature scale is condensed. Modified after Naeser (1979).

properties, the sample ages should decrease systematically to a depth that corresponds to the total annealing temperature for that apatite composition (~100–150 °C). This region between no annealing and total annealing is termed the partial annealing zone (PAZ). At greater depth and at higher temperatures, fission-tracks should be totally annealed and AFT ages should be zero (Fig. 2a). Examples of borehole AFT age profiles that exhibit equilibrated maximum temperature profiles include the Otway Basin, Australia (Gleadow and Duddy 1981; Gleadow et al. 1983; Green et al. 1989a) and the San Joaquin Valley, California (Naeser et al. 1990).

If a sedimentary section is uplifted toward the erosional surface (exhumed) after maximum burial, the former zone of total annealing and the PAZ are uplifted as well. Uplifted apatites from former totally annealed (zero age) and partially annealed depths will begin to accumulate tracks thus increasing the ages in these sections to form a fossil total annealing zone and a fossil partial annealing zone (Fig. 2b) (Naeser 1979; Gleadow et al. 1983; Gleadow and Fitzgerald 1987; Fitzgerald and Gleadow 1990). It should be noted that it is rare to have both a fossil and modern PAZ preserved in a borehole profile because most wells are too shallow. Fossil PAZs and the break in slope generally are observed in surface sample age versus elevation transects (e.g., Fitzgerald and Gleadow 1990) whereas the base of the fossil total annealing zone is preserved in well sections.

Fission-track length data provide important constraints in the thermal history assessment of sedimentary basins. Track length distributions, in combination with apparent fission-track ages, allow a basin analyst to discriminate between different thermal history scenarios. Although extremely simplistic, Figure 3 illustrates seven possible example thermal histories for sedimentary strata derived from a single monocompositional source and their characteristic track length distributions. Paths 1–3 show progressive burial to maximum depths below the top of the PAZ followed by near isothermal conditions. The shallowest sample (path 1) shows long track lengths with narrow distributions indicative of that sample's grains not being annealed

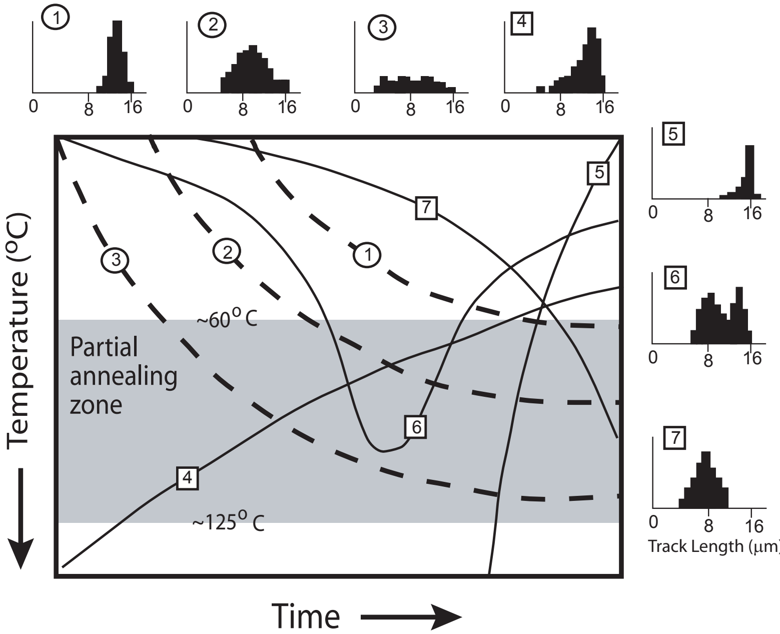

Figure 3. Schematic burial/temperature histories and representative track length distributions. Paths 1-3 show heating followed by nearly isothermal conditions in the apatite partial annealing zone. Paths 4 and 5 show heating from temperatures greater than the base of the partial annealing zone. Path 6 shows heating into the partial annealing zone followed by cooling out of it. Path 7 shows rapid heating to temperatures in the partial annealing zone. Modified after Gleadow et al. (1983).

after deposition. With greater depth (and temperature) the average track lengths progressively get shorter and the distribution of tracks spreads out reflecting the partial annealing. The amount of spread in these paths could be more than illustrated if detrital grains were from multiple sources or had different compositions. Paths 4 and 5 show cooling from depths within or below the PAZ. With cooling from temperatures above the base of the PAZ for this apatite species, average track lengths tend to be long but with negative skewness (path 4 and 5), but the distribution gets narrower with more rapid cooling through the PAZ—compare path 4 with 5. For a sample that is heated to PAZ temperatures and then cooled (path 6), a bimodal distribution can be expected because tracks that were shortened while the sample was in the PAZ are mixed with longer tracks that formed after cooling out of the PAZ. For samples that have experienced relatively recent and rapid heating to maximum temperatures (path 7), average track lengths will be relatively short but not as spread out as in the case of longer periods of time in the PAZ (paths 2 and 3).

In the last decade and a half, several computer programs have been developed (e.g., Green et al. 1989b; Corrigan 1991; Crowley 1993; Gallagher 1995; Willett 1997; Ketcham et al. 2000; Issler 2004) to compute thermal histories from AFT age and track length data. Most of these programs are based on annealing models that assume a single composition for apatite grains (e.g., Laslett et al. 1987; Crowley et al. 1991), but the program (AFTSolve) of Ketcham et al. (2000) is based on multi-kinetic and/or multi-compositional models—see Donelick et al. (2005) and Ketcham (2005) in this volume for detailed discussions.

Apatite composition strongly affects the annealing characteristics of individual apatite grains (e.g., Green et al. 1985). Chlorine-rich apatites tend to anneal more slowly than fluorine-rich apatites, thus the temperature for total annealing is greater for chlorine-rich apatites than for fluorine-rich. This is particularly important in sedimentary basins because grains can come from a variety of sources with different compositions. A substantial advancement in our ability to utilize apatite fission-track data in the last decade has been the realization that apatite fission track analyses should be done in combination with some measurement of composition. In some studies, each dated grain in AFT samples have been microprobed for composition to make direct comparisons between grain ages and chemistry (e.g., O'Sullivan and Brown 1998; Crowhurst et al. 2002; Lorencak et al. 2004). Recently, labs have started to routinely assess relative composition between apatites by measuring the etch pit width parallel to the crystallographic *c*-axis (D_{par}) (e.g., Burtner et al. 1994; Ketcham et al. 1999; Donelick et al. 2005). The utility of measuring D_{par} is that it is straightforward to measure on dated grains, is less expensive than microprobe analysis, and there is publicly available software that allows easy incorporation of D_{par} data—see Donelick et al. (2005) and Ketcham (2005) in this volume for review. Calibrated kinetics (composition or D_{par}) can now routinely be incorporated into quantitative thermal history models (e.g., Ketcham et al. 1999, 2000; Ketcham 2005). The ease of generating compositional information from D_{par} and its incorporation in modeling programs allows the basin analyst to more rigorously evaluate potential thermal histories from AFT data.

Because apatite grains in sedimentary basins can be derived from multiple sources, from a single source with a complicated cooling history, and/or have a range of compositions, it is useful to evaluate the sample for heterogeneous age distributions, especially in samples from the upper part or above the PAZ. Radial plots (Galbraith 1990) are useful for visualizing different age populations in a set of single grain ages. Figure 4 shows an example radial plot from a surface sample in northern Scotland (Carter 1999). O'Sullivan and Parrish (1995) illustrate simple cases (their Fig. 7) of single grain age distributions on radial plots for different positions relative to the PAZ. They show that samples from the PAZ tend to have a fanning out pattern of ages, or "open jaw", reflecting a wide spread in single grain ages. Samples from below or above the PAZ would tend to have narrower distributions of single grain ages. In the example shown in Figure 4, a central age of 320 Ma is shown by the horizontal line extending to the radial part of the plot at the right. Extrapolation of a line from the origin to the radial arc gives the age of each grain. Single grain ages that lie far from the horizontal line, especially outside of the ± 2σ intervals on the *y*-axis, may belong to other age modes than the one suggested by the central age. Several methods for decomposing fission-track ages using peak-fitting methods are available (e.g., Galbraith and Green 1990; Brandon 1992; Sambridge and Compston 1994). In the case of Figure 4, two additional age components of 206 and 557 Ma were recognized by Carter (1999), who used annealing models to interpret the age components as representing slow cooling of the source region through the PAZ starting prior to 500 Ma, and rapid cooling through the apatite PAZ at about 200 Ma. This example is one

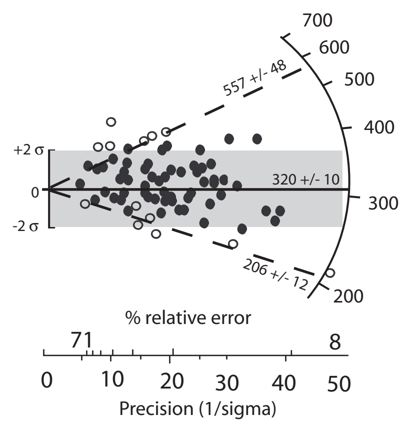

Figure 4. Radial plot showing spread in apatite single grain age data. A central age (Galbraith and Laslett 1993) of 320 Ma is shown by the horizontal line extending to the radial part of the plot at the right. The *x*-axis shows the normalized uncertainty (% error) of each grain age and the y-axis shows the 2σ uncertainty normalized to the length of the scale on the *y*-axis. Filled dots represent ages that fit one age population. Trends of open circles that bound the dots are interpreted to represent additional age populations (see text). Modified after Carter (1999).

that shows that sedimentary basin AFT data can provide powerful constraints not only on the thermal evolution (burial and exhumation) of the depositional basin, but also on source region exhumation rates and timing (see later section) and on tectonic processes that lead to the basin formation.

Apatite (U-Th)/He dating

One of the major advancements in low-temperature thermochronology over the last decade has been use of apatite (U-Th)/He dating. Reviews of the methods and uses of apatite helium are given by Farley (2002) and Ehlers and Farley (2003). The method is based on the production of helium from isotopes of uranium and thorium, but the partial loss of helium due to diffusion out of the crystals has lead to the realization that the method can be used as a thermochronometer (e.g., Zeitler et al. 1987; Lippolt et al. 1994; Wolf et al. 1996). Systematic diffusion studies (Wolf et al. 1996; Farley 2000) indicate that apatite He ages provide thermochronologic information for temperatures between approximately 40–75 °C; at geologic time scales helium is completely diffused from apatite at >75 °C and nearly all the helium is retained at <40 °C. Thus apatite He ages potentially provide lower temperature thermochronologic constraints than that of apatite fission-track ages.

The expected apatite He age profile in a borehole sequence where maximum temperatures have been attained is similar to that of the AFT profile, except that temperatures for any age greater than zero is lower for He ages than for AFT ages (Fig. 2a). The region between about 40–75 °C is referred to as the helium partial retention zone (HePRZ). He ages at depths below the base of the HePRZ are zero and above the HePRZ they are governed by the detrital He ages, which can show considerable spread if there are variable sources. Like the AFT age profile in Figure 2b, during exhumation of the section the He profile is shifted upward so that a new HePRZ and a fossil HePRZ are established as helium accumulates. In one example, paired AFT and apatite He ages from a tilted fault block in the White Mountains (California) confirm a paired fossil HePRZ and PAZ (Stockli et al. 2000).

Wolf et al. (1998) developed a mathematical model to evaluate the time-temperature sensitivity of helium diffusion. The size of grains affects the He age such that larger grains are expected to give older ages, especially in cases of slow cooling (Farley 2000; Reiners and Farley 2001). Helium age modeling with grain size effects is now routinely used to compute model He ages from temperature histories; forward and inverse modeling schemes are discussed by Ketcham (2005) in this volume.

A study in the Otway Basin of Australia (House et al. 1999) showed that He ages from boreholes decrease from about 75 Ma at the surface to nearly zero at depths where temperature is approximately 80 °C. This He age versus temperature profile is consistent with a HePRZ discussed above and with predictions from laboratory data (Wolf et al. 1996). However, the measured He age profile is not consistent with one predicted from a thermal history based mainly on published AFT and vitrinite reflectance data. House et al. (2002) integrated detailed apatite He age data with new and old AFT data from Otway Basin to address these discrepancies and to reevaluate its thermal history. Figure 5 shows that Otway Basin He and AFT ages decrease with increasing temperature and that at any temperature the AFT ages are greater than the He ages. There is considerable scatter in the data, but a positive correlation between grain size and He age suggests that the scatter in the He ages may be caused by grain size effects and the scatter in the AFT ages is shown to be caused by variations in apatite grain composition (House et al. 2002). Model He age versus depth profiles computed from published thermal histories, which are based on burial models and AFT and vitrinite reflectance constraints (e.g., Duddy 1994), are generally similar to measured He age versus depth profiles for eastern part of the Otway Basin. In the western part of the basin, the model He ages are as much as 40 Ma older than measured ages at the same temperature (Fig. 5). House et al. (2002)

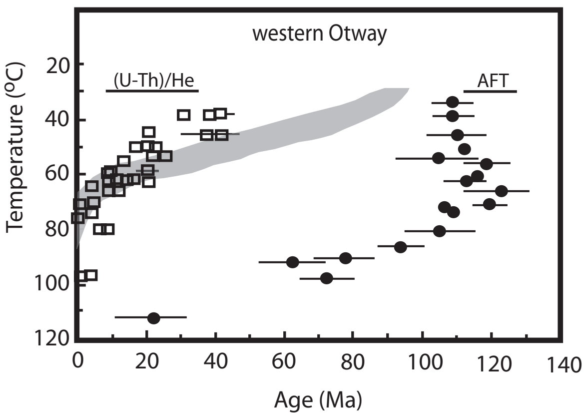

Figure 5. Apatite fission-track (dots) and (U-Th)/He (squares) ages versus present-day temperature for wells from the western part of the Otway Basin in southeast Australia. Shaded region represents model (U-Th)/He ages based on published thermal histories from fission-track data. The misfit of the model and measured He ages suggests that temperatures were greater in the past than indicated by fission-track data alone. Modified after House et al. (2002).

interpret the mismatch of the model and predicted He data to be the result of slightly higher temperatures due to higher geothermal gradients during the Cenozoic, perhaps related to fluid flow. The He age data in this case allowed the thermal history the Otway Basin to be refined and better constrained when compared to models based purely on the higher temperature apatite fission-track data. This study, as well as others (e.g., Crowhurst et al. 2002; Lorancak et al. 2004), points to the effectiveness of extracting more information from sedimentary basins by combining multiple low-temperature thermochronometer data sets.

Combining apatite fission-track and other thermal indicators

In the last decade AFT analysis has been combined with maximum paleotemperature indicators such as vitrinite reflectance (e.g., Bray et al. 1992; Arne and Zentilli 1994; Green et al. 1995; Kamp et al. 1996; O'Sullivan 1999; Marshallsea et al. 2000; Ventura et al. 2001; O'Sullivan and Wallace 2002), fluid inclusions (e.g., Pagell et al. 1997; Parnell et al. 1999), or $^{40}Ar/^{39}Ar$ (e.g., Kohn et al. 1997) to provide stronger and more detailed constraints on thermal histories of sedimentary basins.

Thermochronometers, especially when combined with maximum paleotemperature techniques as listed above, provide some of the best indicators of both magnitude and timing of basin inversion in sedimentary basins (e.g., Kamp and Green 1990; Bray et al. 1992; Green et al. 1995; Hill et al. 1995). Basin inversion is the process of changing from general basin subsidence to local or regional uplift of the sedimentary section. If the overlying strata are removed by erosion during uplift, then the once deeper strata provide a record of the inversion. Bray et al. (1992) outlined a method for using combined AFT and vitrinite reflectance data to estimate amounts of past burial and subsequent inversion. Vitrinite reflectance is a measure of coalification rank of sedimentary organic matter (e.g., Lopatin 1971; Tissot and Welte 1978) and provides a measure of relative maturity that is generally related to depth of burial. More recently, vitrinite reflectance has been quantified so that maximum temperature information can be estimated (Burnham and Sweeney 1989). However, vitrinite reflectance data alone can not provide estimates of the timing of maximum temperatures whereas AFT data can in some cases provide both maximum temperature and its timing. To estimate past burial amounts, computed maximum temperatures from vitrinite reflectance and/or AFT data are plotted as a function of depth and compared to the present-day geothermal gradient (Fig. 6). Projection of the line through the maximum temperature data to the present-day surface temperature provides an estimate of denudation amount. Bray et al. (1992) argue that if the paleotemperature gradient is parallel to the present-day gradient, then paleoheat flow at the time of maximum burial was the

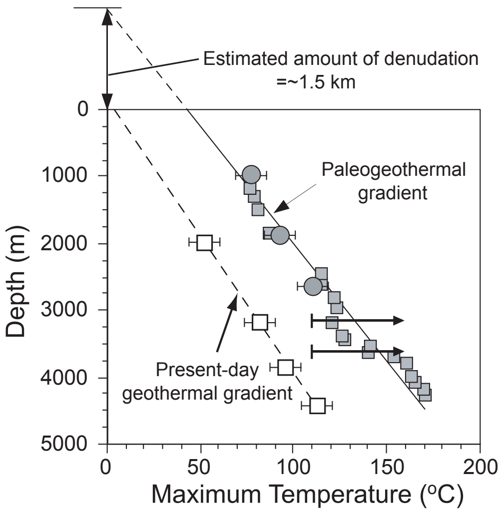

Figure 6. Temperature versus depth plot showing present-day temperatures in a well (open squares) and computed maximum paleotemperatures from vitrinite reflectance (gray squares) and apatite fission-track (gray circles) data. Horizontal arrows indicate that temperatures based on apatite fission-track data were greater than about 110 °C. Lines through the data approximate present-day and paleo temperature gradients. Linear paleotemperature gradients that are parallel to the present gradient suggest paleoheat flow that was similar to heat flow today. In this example, paleoheat flow was similar to present-day. Projection of the paleotemperature gradient to the zero temperature axis gives estimate of vertical uplift and denudation (Bray et al. 1992). Modified after Bray et al. (1992) and O'Sullivan and Wallace (2002).

same as today. If the paleotemperature gradient is greater or less than the present-day profile, then paleoheat flows of greater or less than today, respectively, can be interpreted. Non-linear paleotemperature gradients may indicate higher or lower heat flow through the sediments due to magmatic intrusion or fluid flow (Bray et al. 1992; Duddy et al. 1994).

Higher temperature thermochronometers

Higher temperature thermochronometers such as zircon fission-track dating, $^{40}Ar/^{39}Ar$ dating, and zircon (U-Th)/He dating have been used less extensively than the lower closure temperature systems (apatite fission-track and (U-Th)/He) in evaluating the thermal history of sedimentary basins. The closure temperatures for these systems are ~185–240 °C for zircon fission-track (e.g., Brandon et al. 1998; Tagami et al. 2005), ~350–420 °C for white mica $^{40}Ar/^{39}Ar$ (McDougall and Harrison 1999; Hodges et al. 2005), ~150–200 °C for k-feldspar $^{40}Ar/^{39}Ar$ (Lovera et al. 1997; Harrison et al. 2005), and 180–200 °C for zircon (U-Th)/He (Reiners et al. 2002; Reiners 2005). These higher closure temperatures are less sensitive to typical temperature ranges in most sedimentary basins thus making them ideal for using detrital grains in evaluating source region parameters. A later section of this paper outlines the use of some of these methods.

EXAMPLES OF THERMOCHRONOMETER USE IN SEDIMENTARY BASINS

Thermochronometer data have been used in many studies to evaluate the thermal history of sedimentary basins in the last decade (e.g., Ravenhurst et al. 1994; Green et al. 1995; Sobel and Dumitru 1997; Issler et al. 1999; O'Sullivan 1999; Ventura et al. 2001; Arne et al. 2002; Lim et al. 2003). The intent is not to review all of these, but to offer a few example studies.

Example of a sedimentary basin thermal history – the Williston Basin

Williston Basin is a continental interior epicratonic basin (~800 km diameter) that straddles the Canada-United states boundary and that formed dominantly in the Paleozoic (Osadetz et al. 2002 and references therein). Subsidence in the basin has been described as monotonic and persistent (e.g., Ahern and Mrkvicka 1984) as well as containing rapid subsidence phases (e.g., Burgess et al. 1997). Rocks of the Williston basin and surrounding region consist of Precambrian basement overlain by Paleozoic, Mesozoic, and Cenozoic sediments. The Paleozoic strata consist of carbonates, clastics, and organic-rich mudstone and shale. The preserved cumulative stratigraphic thickness ranges up to about 5 km. The Canadian Williston basin is an important hydrocarbon basin and is the region where the petroleum system concept was first described (Dow 1974).

Osadetz et al. (2002) evaluated apatite fission-track data from Precambrian basement rocks collected from drill holes distributed throughout the Canadian part of the basin (Fig. 7). The basement rocks underlie the Phanerazoic strata at depths as great as 3 km. In most of the study region, the temperature at the top of the Precambrian basement is <70 °C, well below the total annealing temperature of fission tracks in apatite. Surface heat flow typically ranges from about 40–60 mW/m^2. Two regions on the east and west sides of the basin give AFT ages ~350–450 Ma with an area of 250–300 Ma ages in between. The southern part of the basin has ages of <100 Ma. The chlorine content of nearly all probed grains was <0.2 wt% Cl indicating that the apatites are mostly fluorine-rich. Osadetz et al. (2002) argue that the annealing model of Laslett et al. (1987) could be used to evaluate thermal histories, though that particular annealing model is based on a higher chlorine content of ~0.4 wt% for Durango apatite. Thus, the estimated paleotemperatures described below should be considered maximum estimates; the overall interpretations for elevated paleoheat flow in the late Paleozoic discussed below should not change.

Figure 8 shows two representative thermal histories for samples collected in different parts of the basin (Fig. 7). These thermal histories were generated using the program "Monte Trax" described by Gallagher (1995), which uses a Monte Carlo approach to invert for thermal histories that satisfy the fission-track ages and length distributions. The main features of these two simulations, which are similar to those from other wells, are the cooling events from elevated temperatures in the late Paleozoic (~245–365 Ma) and in the Late Cretaceous-Paleogene (~75–50 Ma). In the Lashburn well (Fig. 8), temperatures reached ~85 °C and well within the apatite partial annealing zone in the late Paleozoic. This heating was followed by

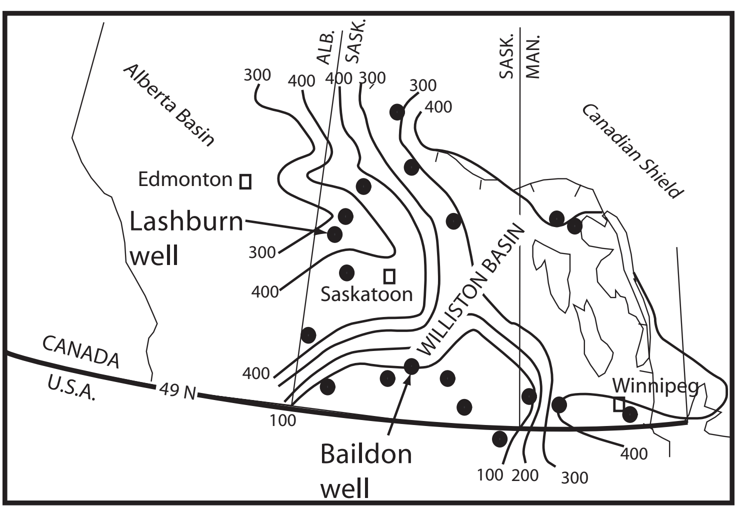

Figure 7. Map showing location of Williston Basin in Canada and United States. Dots show locations of wells that penetrate to basement. Wells "Lashburn" and "Baildon" are discussed in text and in Figure 8. Contours are apatite fission-track ages for basement samples. Modified after Osadetz et al. (2002).

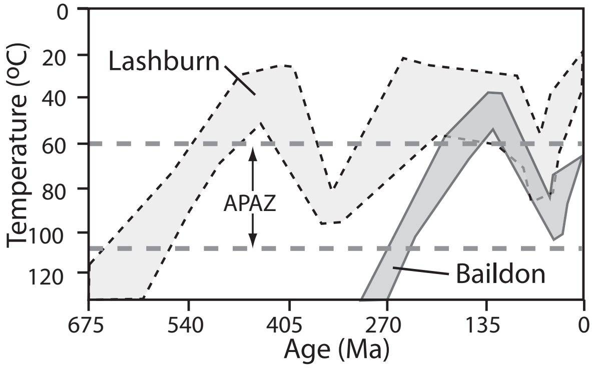

Figure 8. Thermal histories based on apatite fission-track data from basement samples in "Lashburn" and "Baildon" wells in Williston Basin—see Figure 7 for locations. APAZ is apatite partial annealing zone. Thermal histories computed using Monte Trax program described by Gallagher (1995). Modified after Osadetz et al. (2002).

an episode of cooling, then additional heating in the Late Cretaceous. In the Baildon well, temperatures were greater than 120 °C in the late Paleozoic, decreased to about 50 °C in the Cretaceous, and increased again at the end of the Cretaceous. Thus, in both wells the basement samples would have been partially or completely annealed during the late Paleozoic.

A burial history was constructed from known regional stratigraphic thicknesses for the area around the Baildon well (Fig. 9). Only the top of the basement horizon is shown in Figure 9, but it is clear that the maximum burial occurred in the Late Cretaceous – Early Tertiary when basin depths reached about 3 km. During the time period when fission-track models indicate temperatures >120 °C in the late Paleozoic, maximum burial depths were <2 km. For heat

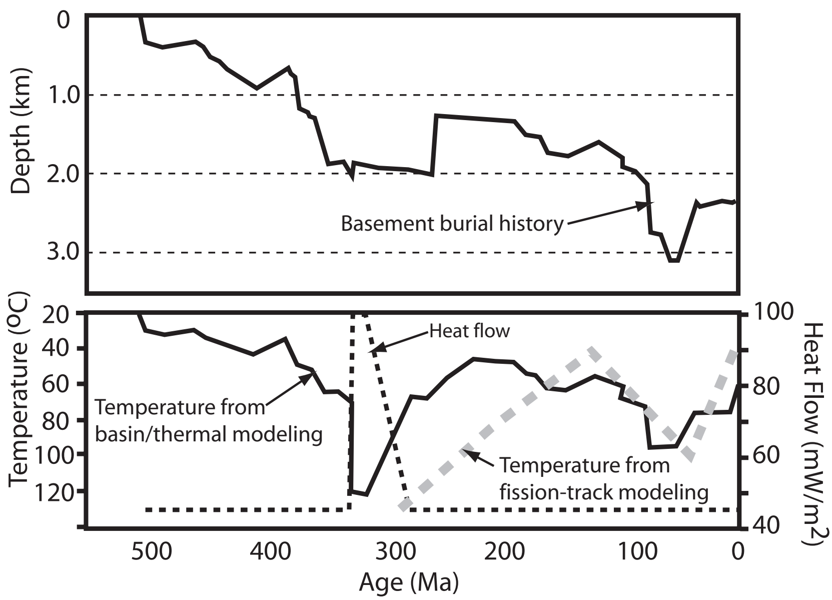

Figure 9. Upper plot shows basement burial history for the Baildon well in Williston Basin. Lower plot shows temperature history based on the burial history and the heat flow condition that includes high heat flow in late Paleozoic (dashed thin line). Thick gray dashed curve in lower plot is acceptable temperature history from fission-track modeling. Modified after Osadetz et al. (2002).

flow values similar to those at present, temperatures must have been on the order of 50–60 °C at these depths. Clearly, the fission-track data require higher heat flow and higher geothermal gradients during the late Paleozoic; nearly 100 mW/m^2, or nearly twice the present-day heat flow, is necessary in the late Paleozoic in order to increase basin temperatures at this time and to satisfy the fission-track constraints. Osadetz et al. (2002) used a basin modeling program (BasinMod™) to construct a temperature history based on the burial history of the well and the proposed heat flow history (Fig. 9). The computed temperature history (solid curve in lower plot of Fig. 9) shows temperatures of ~120 °C in the late Paleozoic and ~90 °C in the Late Cretaceous-Early Tertiary; this temperature history is very similar to that required by the fission-track data in the well. Therefore a varying heat flow history that was significantly elevated in the late Paleozoic was interpreted for the Williston Basin by Osadetz et al. (2002).

The elevated late Paleozoic heat flow has significant implications for the petroleum system in the basin as well as its geodynamic history. The fission-track data and modeling imply that the lower Paleozoic source rocks in the basin would have been in the oil window in the late Paleozoic, which is quite different from previous models that place the earliest hydrocarbon generation in the Late Cretaceous. Osadetz et al. (2002) proposed that the high heat flow was caused by dynamic mantle upwelling starting in the middle Devonian, which caused lithospheric weakening that lead to the rapid subsidence seen at ~400 Ma in Figure 9.

Example integrating burial history with AFT data in an active-margin basin

Taranaki Basin is located both onshore and offshore along the western side of the North Island of New Zealand (Fig. 10), straddles the plate-boundary zone between the Indo-Australian plate and the Pacific plate, and has been variably affected by plate-boundary deformation during Neogene to Recent times. The basin initially developed during the Cretaceous by a rifting event that separated New Zealand from Australia resulting in extensive deposition in fault-controlled sub-basins (King and Thrasher 1996). The deep (>5.5 km) petroleum well Kapuni Deep-1 is located onshore in Taranaki Basin (Fig. 10) and is chosen as a test case for discussion of thermal history modeling combined with thermochronometer data and detailed basin modeling.

Figure 10 shows a burial-thermal history for Kapuni Deep-1 using input constraints that include: (1) burial history from detailed well and seismic data; (2) thermal properties for all sedimentary units; (3) porosity-depth relations; and (4) estimates of paleo-surface temperature based on oxygen isotope and paleontologic evidence. A one-dimensional finite element model ("Bassim" modified from Willett 1988) was used to compute the transient conductive thermal field during sediment deposition and erosion, sediment compaction, sill intrusion, thrusting, and syndepositional and synerosional crustal thickening and thinning (Armstrong et al. 1996). The lower model boundary condition (basal heat flow) was placed at a depth of 40 km to couple basin thermal effects to deeper thermal conditions.

Initial conditions include Late Cretaceous rifting (Weissel and Hayes 1977; Armstrong et al. 1996), which caused initial rapid subsidence and as much as 5 km of Upper Cretaceous-Paleocene sediments to be deposited (Fig. 10). Slower subsidence followed until the late Miocene, when ~300 m of denudation occurred due to uplift along local faults. Rapid subsidence ensued during the Pliocene, followed by ~500 m of rapid Pleistocene erosion during North Island uplift.

Bottom-hole temperatures in the well increase systematically to a depth of about 4.5 km where the down-hole gradient increases. Apatite fission-track ages show a very rapid change from >80 Ma at depths of about 3.5 km to <1 Ma at 5.2 km depth (Fig. 10). Chlorine contents from the three deepest samples average 0.3 wt.%, with 75% having less than 0.4 wt.%, but not all dated grains were probed; if this study were done today, each grain would be analyzed

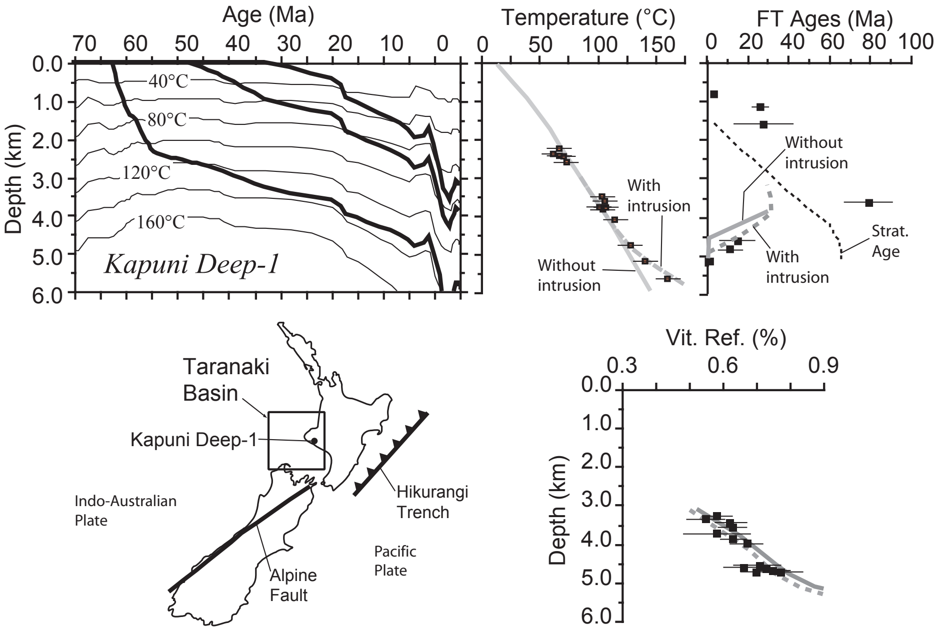

Figure 10. Burial/thermal history and output parameters temperature, apatite fission-track, and vitrinite reflectance data for well Kapuni Deep-1 in Taranaki Basin, New Zealand. Burial history shows three stratigraphic horizons (bold curves) and isotherms (thin curves). Solid curves in the temperature, fission-track, and vitrinite reflectance plots are model values for case of tracking thermal history with burial and erosion only. Thick dashed curves are for case of including sill intrusion below the sediments in the last <1 M.y. Map shows Taranaki Basin in New Zealand in relation to the plate tectonic configuration and well location discussed in this paper. Modified after Armstrong et al. (1996).

using D_{par} as a proxy for composition as discussed earlier. Thus, the interpretations listed below are acceptable, but may not be the only acceptable ones. The >80 Ma sample is older than the stratigraphic age indicating that its age reflects a significant provenance signal and that it has not been substantially reset since the Late Cretaceous. At depths of 4.7 km the AFT ages are ~15 Ma, yet the temperature is 120–125 °C; apatites typical of most grains in Taranaki Basin should be completely annealed if temperature is held at these temperatures for significant time. The three deepest samples may be part of a relatively narrow partial annealing zone (<1000 m wide); this interpretation is consistent with a high geothermal gradient in the deeper parts of the section, as is presently the case in the well. Vitrinite reflectance increases systematically with depth from 0.5% to 0.8%.

The annealing model of Willett (1992), which uses the Arrhenius model of Crowley et al. (1991), was used to predict the AFT ages and the model of Burnham and Sweeney (1989) was used to predict vitrinite reflectance for the burial history. The solid curves in the temperature, AFT age, and vitrinite reflectance plots (Fig. 10) show the model results for the case of tracking temperature change with burial and erosion only. The modeled present-day temperatures do not show the increase in gradient in the deeper parts of the well. Modeled fission-track ages are completely annealed (zero age) at 4.6 km where measured age is 16 Ma. Apatite compositions suggest that the apparently old AFT ages are not related to high chlorine composition.

To account for increased temperature gradient and the poor fit to the AFT data, a simulation was ran that includes shallow intrusion in the last <1 Ma (Armstrong et al. 1997). An intrusion model is reasonable for this area because the Kapuni Deep-1 well is in line with and in the direction of a younging set of Quaternary volcanic edifices on the Taranaki Peninsula. Intrusion associated with the volcanic activity may be responsible for locally high heat flow farther north on the peninsula (Funnell et al. 1996). The intrusion model includes the transient thermal effects of instantaneous horizontal sill intrusion as outlined by Ehlers (2005) and shows good fits to both the temperature and AFT data (Fig. 10). Vitrinite reflectance data show essentially the same fit with both the intrusion and non-intrusion model, indicating that the vitrinite reflectance data are less sensitive to the short-term transient thermal effects than are the AFT data. The interpretation is that both data sets (temperature and AFT) are being affected by a thermal wave propagating up from below; given enough time, the increased temperature gradient will smooth out and the AFT samples at >4.5 km will be completely annealed.

This example illustrates the power and importance of utilizing multiple data sets and basin modeling techniques to extract a detailed thermal history from sedimentary basins. However, additional low-temperature thermochronometer data from apatite (U-Th)/He dating and additional kinetic data on all AFT-dated grains would help constrain the timing of potential intrusion heating further, or provide insight into other potential interpretations that may not include intrusion at all.

A complex history example – constraining structures with outcrop and well data

Low-temperature thermochronometry data from sedimentary basins are commonly used to back-out complex structural histories from both well and outcrop samples. One such case history, based on the work of O'Sullivan and Wallace (2002), in the E-W trending Sadlerochit Mountains of the northeastern Brooks Range (Fig. 11), northern Alaska is illustrated below. The northeastern Brooks Range has been intensely folded by a series of deformational events probably associated with convergence between the North America and Pacific Plates about 1200 km to the south.

Deformation in the main part of the Brooks Range included shortening associated with multiple allochthon emplacements in the late Mesozoic. This shortening is thought to have propogated northward into the Sadlerochit Mountains area in the Paleocene and Eocene. Structures of the northeastern Brooks Range generally comprise a set of north-verging folds and thrusts that form a complex array of fault-bend folds, fault-propagation folds, duplexes, and horses. However, the sequence and timing of thrusting in the Sadlerochit Mountains are poorly constrained because syn- and post-tectonic deposits that could be used to date the deformation are lacking. The goal of evaluating fission-track data from deformed sedimentary basin strata, in combination with complex fault/fold relations and vitrinite reflectance data, is to place constraints on the timing and sequence of fault/fold development and their relations to basement involvement in the deformation style.

O'Sullivan and Wallace (2002) present an extensive fission-track data set for the region around the Sadlerochit Mountains and from one well located ~20 km west of and along trend with the Sadlerochit Mountains. Only a subset of the outcrop data are discussed here. Figure 12 shows apatite and zircon fission-track ages for from Triassic–Tertiary age clastic sediments from the north flank of the Sadlerochit Mountains. The data are plotted to represent a stack of upward-younging sediments as if they were collected from a well. The apatite fission-track ages are all younger than their respective stratigraphic ages, but converge toward the stratigraphic age up-section. The upper part of the section yields AFT ages of 44–51 Ma and the lower section yields ages of 26–31 Ma (Fig. 12). Mean track lengths are 14.8 ± 0.1 to 13.9 ± 0.1 μm. Track length distributions are very narrow, with slight tails to shorter track lengths (Fig. 12), indicating that all samples cooled quickly through the apatite partial annealing zone (Fig. 3). Apatite composition was determined via microprobe on a subset of the grains; all the grains probed had <0.4 wt.% Cl indicating a dominantly fluorine-rich apatite

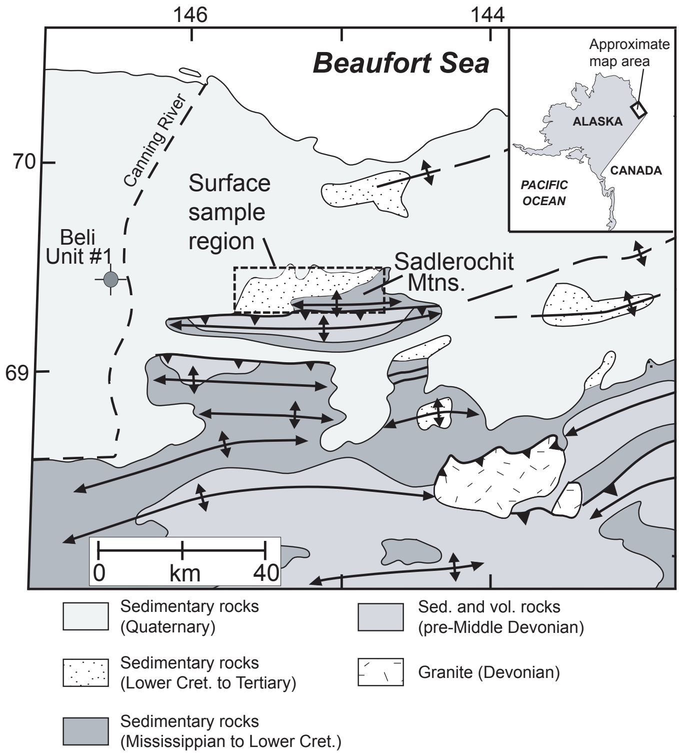

Figure 11. Generalized geologic map showing the locations of the Sadlerochit Mountains and well Beli Unit#1 in northern Alaska. Arrowed curves show locations of major anticlines. Modified after O'Sullivan and Wallace (2002).

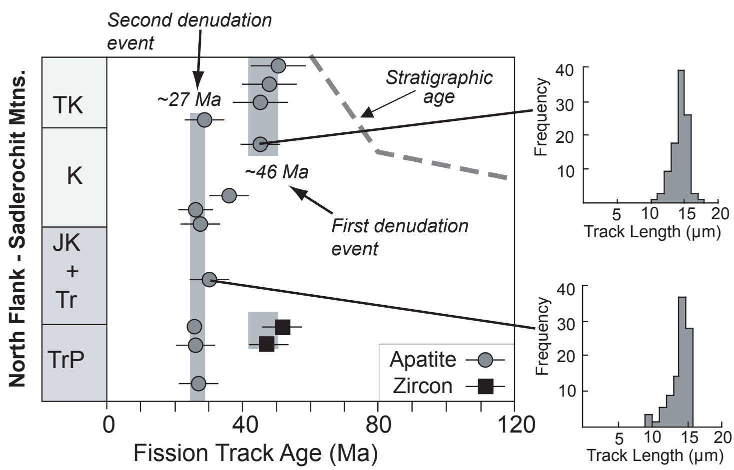

Figure 12. Fission-track data for the north flank of the Sadlerochit Mountains. See Figure 11 for sampling area. T=Tertiary, K=Cretaceous, J=Jurassic, Tr=Triassic, P=Permian. Modified after O'Sullivan and Wallace (2002).

population. Modeling of the age and track length distributions using the annealing model of Laslett et al. (1987) for fluorine-rich apatites indicates that the upper section cooled rapidly to temperatures of less than 50 °C at ~45 Ma. The deeper samples at that time were still hotter than ~110 °C until 27 Ma when they rapidly cooled to less than 50 °C. As the authors point out, the estimated paleotemperatures should be interpreted as maximum values because the actual chlorine contents are less than the 0.4 wt.% used in the Laslett et al. (1987) model.

Two samples in the deeper part of the section yield zircon fission-track ages of 51 Ma and 47 Ma. These ages are much younger than their stratigraphic ages (Fig. 12), thus indicating at least partial resetting of some grains. Assuming a partial annealing temperature range of ~180 to 225 °C for zircon fission tracks, the samples deeper in the section would have cooled to between 180–225 °C and ~110 °C about the 47–50 Ma, approximately the same time as the upper samples cooled to less than 50 °C.

Samples from the well Beli Unit #1, which is located west of and along strike with the Sadlerochit Mountains (Fig. 11) yield ages that decrease with increasing depth. The three deepest samples are younger than the stratigraphic ages, decrease with increasing depth from 52–8 Ma, and are all within the partial annealing zone. Mean track lengths for two of the deepest samples are ~10.6–11.8 μm and distributions are fairly wide, which is characteristic of samples that are within, and perhaps near the base of, the partial annealing zone. Annealing modeling reveals that these samples rapidly cooled 35–45 °C from maximum temperatures of 110 °C about 40–50 Ma. This cooling amount corresponds to ~1.3–1.8 km of depth difference assuming typical geothermal gradient of 27 °C/km. The timing of cooling is concordant with the early phase of cooling in the Sadlerochit Mountains discussed earlier based on surface samples.

Maximum paleotemperatures from the vitrinite reflectance data combined with estimates of paleotemperature from apatite fission-track data in well Beli Unit #1 clearly show a linear trend offset from the present-day temperature gradient (Fig. 6). The offset paleogeothermal gradient line suggests ~1.5 km of exhumation at the well location west of the Sadlerochit Mountains.

The combined apatite fission-track, zircon fission-track, and vitrinite reflectance results from outcrop and well samples indicates two major rapid cooling periods that are interpreted to be the result of major denudation events. These include: (1) approximately 2 km of unroofing at ~45 Ma in the Sadlerochit Mountains and (2) a second rapid cooling event that occurred ~27 Ma as indicated by the samples from deeper in the section. Assuming a constant geothermal gradient, the deeper samples would have passed rapidly through depths of 2–4 km implying more that 2 km of unroofing during this event.

The preferred model of O'Sullivan and Wallace (2002) is that there were two levels of structural detachment that emplaced basement duplexes at ~45 Ma. This duplexing would have elevated the Sadlerochit region enough to cause >2 km of unroofing above the duplex zone. The later unroofing event at ~27 Ma is interpreted to be caused by additional out-of-sequence back-thrusting above the already established duplex system (see O'Sullivan and Wallace 2002). The results of this study indicate between 4 and 8 km of structural thickening probably due to basement-involved thrust stacking occurred in the middle Tertiary. Thus, the thermochronologic data help to identify structural style and timing in a very complexly deformed sedimentary basin.

Additional illustrative examples of AFT analysis in sedimentary basins

Burtner and Negrini (1994) used apatite fission-track data in combination with organic maturation data (vitrinite reflectance and Rock-Eval pyrolysis) to evaluate the thermal history of the Idaho-Wyoming (western U.S.A.) thrust belt, which formed during the Sevier Orogeny in the late Mesozoic and early Cenozoic. Burtner and Negrini (1994) used the distribution of AFT ages from outcrop and well samples to show that gravity-driven fluid flow was responsible for advecting large amounts of heat from the foreland basin towards the east. The relatively hot fluids disturbed the thermal field and caused early hydrocarbon generation. Later, thrust stacking caused meteoric water recharge in high regions which drove cooling of samples along the western part of the foreland basin. Burtner et al. (1994) used refinements to apatite fission-track methods, mainly by correcting ages based on composition and etch pit width (D_{par}) data, to show that Lower Cretaceous source rocks were heated sufficiently to generate hydrocarbons prior to thrust faulting to the west; thrust faulting generally had been assumed to be the cause of most heating and trap formation in the foreland basin.

Cederbom et al. (2004) used apatite fission-track age data to infer climate-induced exhumation of the European Alps. They evaluated detrital apatite from several foreland basin boreholes located in the North Alpine Foreland Basin of Switzerland. Individual grain ages from samples at any depth in the wells vary considerably, but the pooled ages show a consistent decrease with increasing depth. The pooled ages recorded in the deepest samples are interpreted to reflect the bases of exhumed partial annealing zones. The bases of the exhumed PAZs have mean ages of about 5 Ma suggesting that uplift and exhumation of the section began then. This age corresponds to the timing of increased sediment accumulation in nearby depositional centers and with an intensification of the Atlantic Gulf Stream. The erosional power of the climate intensification increased and led to isostatic rebound and uplift of the Swiss Alps and the proximal foreland basin (Cederbom et al. 2004).

O'Sullivan and Brown (1998) were able to relate known past surface temperature changes to AFT ages near the base of a well on the North Slope of Alaska. Their analysis showed that late Cenozoic mean annual surface temperature changes of 10–20 °C affected AFT grain ages at depths of ~3–4 km. One of the important implications of this study is that the subsurface effects of long-term surface temperature changes must be accounted for, if possible, when estimating exhumation magnitudes from AFT and apatite (U-Th)/He data.

Higher-temperature thermochronometers in sedimentary basins

Higher-temperature thermochronometers, those with closure temperatures of greater than about 150 °C, have been and will continue to be used in sedimentary basin analysis. These methods generally include zircon fission-track (Zeitler et al. 1986; Cerveny et al. 1988; Brandon and Vance 1992; Carter 1999; Garver et al. 1999; Spiegel et al. 2000; Bernet et al. 2001; 2004; Bernet and Garver 2005), $^{40}Ar/^{39}Ar$ on K-feldspar (e,g., Harrison and Be' 1983; Harrison and Burke 1989; Lovera et al. 1997; Mahon et al. 1998; Harrison et al. 2005), $^{40}Ar/^{39}Ar$ on white mica (e.g., Copeland and Harrison 1990; Najman et al. 1997; White et al. 2002; Carrapa et al. 2003; 2004; Hodges et al. 2005) , or zircon (U-Th)/He dating (e.g., Rahl et al. 2003).

Harrison and Burke (1989) provide early examples of using $^{40}Ar/^{39}Ar$ thermochronology on microcline, based on age spectrum work of Harrison and Be' (1983), to demonstrate the utility of extracting thermal history constrains for geodynamic models. More recently, Mahon et al. (1998) applied $^{40}Ar/^{39}Ar$ thermochronometry, using a multi-diffusion domain model and corrected for excess ^{40}Ar, to evaluate detrital K-feldspars from a deep well in the San Joaquin Valley, California. Their results are consistent with roughly linear heating of the sedimentary section during the early and middle Miocene, followed by more rapid heating between 9–6 Ma. The thermal model generated from their $^{40}Ar/^{39}Ar$ study allowed assessment of porosity and insights into the pore fluid evolution in the overlying sediments, which are major hydrocarbon producers in the San Joaquin Valley.

A major advance in the last decade in sedimentary basin thermochronometer utility has been in higher-temperature detrital thermochronometry, which mainly provide information on the provenance region(s) for the sediments. Detrital thermochronometry methods are reviewed in earlier chapters by Bernet and Garver (2005) and Hodges et al. (2005). Apatite fission-track data generally are less useful for detrital studies because of their lower annealing temperatures and larger relative errors on ages, but Carter and Gallagher (2004) argue that useful source region thermal history information can be recovered from samples heated to as high as 100 °C after burial.

Information gleaned from higher-temperature thermochronometry studies generally includes the numbers of source region exhumation episodes as well as their timing and rates of exhumation (e.g., Bernet et al. 2001, Ruiz et al. 2004). The data also can provide information on long-term stability (i.e., steady-state) of landscape in the source region (e.g., Willett and Brandon 2002; Ruiz et al. 2004). Regardless of the method (fission-track, $^{40}Ar/^{39}Ar$, helium), the technique generally involves measuring ages on many detrital grains (50–100) and decomposing the ages into peaks (e.g., Brandon 1992;1996). Figure 13 shows an example from the Olympic sudduction complex where the distribution of ages shows a main peak at 20 Ma and a broad composite peak centered around ~50 Ma. Two smaller peaks are superimposed on the broad peak at ~45 and 60 Ma. The main peaks then are fitted using Gaussian peak fitting to show the best-fit peaks (Fig. 13).

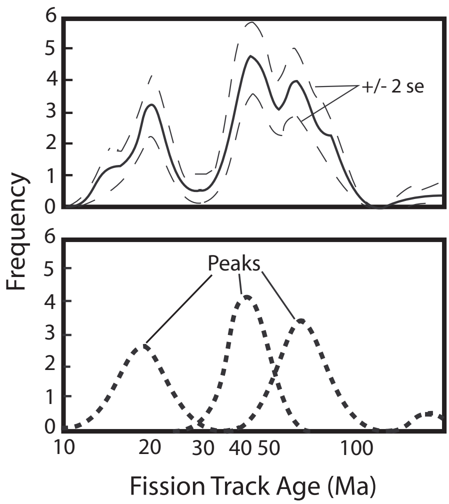

Figure 13. Zircon fission-track age frequency distributions from the Olympic subduction complex with two standard error bounds (upper plot). Lower plot show the age distribution decomposed using Gaussian peak fitting (e.g., Brandon 1992; 1996). Three peaks are present in this example.

Once the peaks are determined from each sample, they can be plotted against known depositional age to determine the "lag time" between when the mineral groups passed through their respective closure temperatures and were deposited in the sedimentary basin. In general, detrital ages increase with increasing depositional age reflecting the sequential exhumation of a source region and burial in the sedimentary basin. Ruiz et al. (2004) define five lag time paths for the relations between detrital age and depositional age. These include the following. (1) Decreasing lag time where the detrital and depositional ages converge up-section. This path indicates increasing source region exhumation with time. (2) Constant lag time where difference in age is constant throughout the section. This path indicates constant source region exhumation rate. (3) Increasing lag time up section, but detrital ages get younger up section. This scenario indicates slowing of exhumation with time. (4) Invariant detrital age up section – indicates major component of volcanic detritus. (5) Detrital ages increase up section. This path indicates possible volcanic contributions, cannibalism of non-reset grains that were deposited previously and re-eroded, and/or changes in source region tectonics.

Figure 14 is an example of detrital zircon fission-track peak ages and their respective depositional ages from the Northern Apennines, Italy (Bernet et al. 2001). The detritus in the sedimentary basin deposits is known to have been derived from the central and western Alps. The angled lines in the plot represent iso-lag time lines; ZFT peak age versus depositional age pairs that plot on one these lines will give the lag time for that sample's time of deposition. In this example, two main source regions are interpreted with lag times of 8 and 16 m.y. The

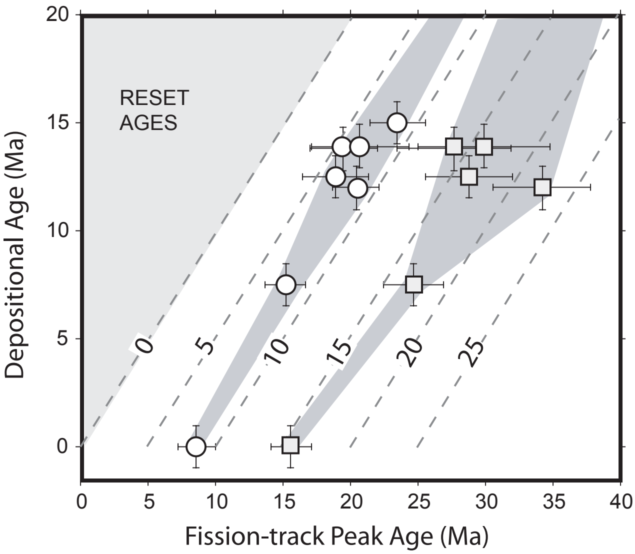

Figure 14. Detrital zircon fission-track peak ages versus depositional age of the stratigraphic unit from which they were extracted in the Northern Appenines, Italy. The area labeled "RESET AGES" represent area where fission-track ages are younger than stratigraphic ages. Diagonal dashed lines represent iso-lag times in million years. In this example, two peak sets are evident at lag times of 8 and 16 m.y. Modified after Bernet et al. (2001).

constant lag time with increasing depositional age for both of the peak sets suggests that the Alps are maintaining exhumational steady-state (Bernet et al. 2001).

Multi-method approaches using different mineral or dating methods are commonly being used to glean more information from detritus in sedimentary basins. Spiegel et al. (2004) use zircon fission-track data in combination with Nd isotope ratios in epidote to evaluate the exhumation history of the central Alps. Carter and Moss (1999) combined U/Pb and zircon fission-track dating to link exhumation and sedimentation in Thailand. Rahl et al. (2003) use zircon (U-Th)/He and U/Pb dating of the same detrital crystals to evaluate source regions for the Navajo Sandstone in Utah.

CONCLUSIONS AND FUTURE DIRECTIONS

Sedimentary basins and their deposits cover most of the solid surface of Earth. The sedimentary layers contain a history of depositional and erosional magnitudes, rates, and timing, which can be combined with modern modeling and thermochronologic techniques to evaluate other factors that influence the basin's history. Low-temperature thermochronometers, mainly apatite fission-track dating, have been used for a couple decades to help constrain thermal histories of sedimentary basins. The last ten years has seen the increased use of apatite fission-track dating in combination with vitrinite reflectance data to provide powerful constraints on past temperature and heat flow changes and magnitude and timing of burial and unroofing events. The temperature changes recorded by the thermochronometers allow assessment of the timing and duration of hydrocarbon production, expulsion, and migration to greatly enhance prospectivity of hydrocarbon systems. Paleoheat flow changes, which can be identified by apatite fission-track parameters, can be used to evaluate tectonic processes responsible for the basin's formation (e.g., Williston Basin). Thermochronometers provide important checks on modeled basin/thermal histories and allow assessment of past temperatures not evident in the present-day temperature field alone. For example, low-temperature thermochronometry data can provide evidence of past localized intrusion or fluid flow events that may have waned after causing basin temperatures to rise or heating that may still be propagating through the basin system. Low-temperature thermochronometers provide important constraints on basin inversion magnitude and timing as well as constraints on timing and style of deformation associated with major tectonic events.

A major advancement in the field of AFT dating has been the appreciation that apatites span a wide range of compositions and that this range in composition leads to a larger range in annealing temperatures than assumed in many studies, from perhaps ~50 °C to ~150 °C. The lower and upper bounds on the PAZ depend on each apatite's composition and kinetic properties. Thus, to extract the most information out of AFT data sets, especially those from sedimentary basins, future studies should include composition/kinetic data on each grain for which an age is determined. Labs have recently begun to assess relative composition/kinetics of apatites by measuring D_{par} (etch pit width parallel the crystallographic *c*-axis). These data should continue to be collected and used in modeling steps to assess acceptable thermal histories.

A significant advance in the last decade has been the combined use of thermochronometers, especially the lowest temperature methods of apatite fission-track and (U-Th)/He dating. The combination of these techniques is already showing great promise in constraining the lowest temperature part of the temperature history. Much effort is being put into combining these techniques, and future directions certainly should include continued efforts to find new ways to integrate these two powerful methods in terms of modeling temperature histories from the collective data sets and finding novel ways of interpreting them. Future directions should also include combined seamless thermochronometer modeling with burial/thermal history modeling in software packages.

The last decade also has seen a growth in using the rich stratigraphic record in sedimentary basins with thermochronometers to assess processes other than the thermal history of the basin itself. The use of higher-temperature thermochronometers such as zircon fission-track, zircon (U-Th)/He, $^{40}Ar/^{39}Ar$, and U-Pb has become increasingly more powerful for assessing source region exhumation events and their causes. These methods are, and will continue to be, used in combination with one another to take advantage of each method's strengths and differences in closure temperatures.

ACKNOWLEDGMENTS

I thank the donors of The Petroleum Research Fund, administered by the American Chemical Society, for support of this effort. S. Perry helped with figure and reference preparation. T. Ehlers, P. Kamp, and, especially, P. O'Sullivan provided reviews of this chapter.

REFERENCES

Ahern JL, Mrkvicka SR (1984) A mechanical and thermal model for the evolution of the Williston Basin. Tectonics 3:79-102

Allen PA, Allen JR (1990) Basin Analysis - Principles and Applications. Blackwell, London

Armstrong PA, Chapman DS (1998) Beyond surface heat flow: An example from a tectonically active sedimentary basin. Geology 26:183-186

Armstrong PA, Chapman DS, Funnell RH, Allis RG, Kamp PJJ (1996) Thermal modelling and hydrocarbon generation in an active-margin basin: The Taranaki basin, New Zealand. Am Assoc Petrol Geol Bull 80: 1216-1241

Armstrong PA, Kamp PJJ, Allis RG, Chapman DS (1997) Thermal effects of intrusion below the Taranaki basin (New Zealand): Evidence from combined apatite fission track age and vitrinite reflectance data. Basin Research 9:151-169

Arne D, Zentilli M (1994) Apatite fission track thermochronology integrated with vitrinite reflectance. *In*: Vitrinite reflectance as a maturity parameter. Mukhopadhyay PK,Dow WG (eds) American Chemical Society, Washington, DC, p 250-268

Arne DC, Grist AM, Zentilli M, Collins M, Embry A, Gentzis T (2002) Cooling of the Sverdrup Basin during Tertiary basin inversion: implications for hydrocarbon exploration. Basin Res 14:183-206

Bally AW, Snelson S (1980) Realms of subsidence. *In*: Facts and Prinicples of World Petroleum Occurrence. Miall AD (ed) Canadian Society of Petroleum Geologists, p 9-79

Bernet M, Brandon MT, Garver JI, Molitor BR (2004) Fundamentals of detrital zircon fission-track analysis for provenance and exhumation studies with examples from the European Alps. *In*: Detrital Thermochronology: Provenance Analysis, Exhumation, and Landscape Evolution of Mountain Belts. Bernet M, Spiegel C (eds) The Geological Society of America, p 25-36

Bernet M, Garver JI (2005) Fission-track analysis of detrital zircon. Rev Mineral Geochem 58:205-238

Bernet M, Zattin M, Garver JI, Brandon MT, Vance JA (2001) Steady-state exhumation of the European Alps. Geology 29:35-38

Brandon MT (1992) Decomposition of fission-track grain age distributions. Am J Sci 292:535-564

Brandon MT (1996) Probability density plot for fission-track grain-age samples. Rad Meas 26:663-676

Brandon MT, Roden-Tice MK, Garver JI (1998) Late Cenozoic exhumation of the Cascadia accretionary wedge in the Olympic Mountains, northwest Washington State. Geol Soc Am Bull 110:985-1009

Brandon MT, Vance JA (1992) New statistical methods for analysis of FT grain age distributions with applications to detrital zircon ages from the Olympic subduction complex, western Washington State. Am J Sci 292:565-636

Bray RJ, Green PF, Duddy IR (1992) Thermal history reconstruction using apatite fission track analysis and vitrinite reflectance: a case study from the UK East Midlands and Southern North Sea. *In*: Exploration Britain: Geological insights for the next decade. Hardman RFP (ed) Geological Society, p 3-25

Burgess P, Gurnis M, Moresi L (1997) Formation of sequences in the cratonic interior of North America by interaction between mantle, eustatic, and stratigraphic process. Geol Soc Am Bull 108:1515-1535

Burnham AK, Sweeney JJ (1989) A chemical kinetic model of vitrinite maturation and reflectance. Geochim Cosmochim Acta 53:2649-2657

Burtner RL, Negrini A (1994) Thermochronology of the Idaho-Wyoming thrust belt during the Sevier Orogeny: A new, calibrated, multiprocess model. Am Assoc Petrol Geol Bull 78:1586-1612

Burtner RL, Nigrini A, Donelick RA (1994) Thermochronology of Lower Cretaceous source rocks in the Idaho-Wyoming Thrust belt. Am Assoc Petrol Geol Bull 78:1613-1636

Carrapa B, Wijbrans J, Bertotti G (2003) Episodic exhumation in the Western Alps. Geology 31:601-604

Carrapa B, Wijbrans J, Bertotti G (2004) Detecting provenance variations and cooling patterns within the western Alpine orogen through 40Ar/39Ar geochronology on detrital sediments: The Tertiary Piedmont Basin, northwest Italy. *In*: Detrital Thermochronology: Provenance Analysis, Exhumation, and Landscape Evolution of Mountain Belts. Bernet M, Spiegel C (eds) Geological Society of America, p 67-84

Carter A (1999) Present status and future avenues of source region discrimination and characterization using fission track analysis. J Sed Geol 124:31-45

Carter A, Gallagher K (2004) Characterizing the significance of provenance on the inference of thermal history models from apatite fission-track data-A synthetic data study. *In*: Detrital Thermochronology: Provenance Analysis, Exhumation, and Landscape Evolution of Mountain Belts. Bernet M, Spiegel C (eds) Geological Society of America, p 7-24

Carter A, Moss SJ (1999) Combined detrital-zircon fission-track and U-Pb dating: a new approach to understanding hinterland evolution. Geology 27:235-238

Cederbom CE, Sinclair HD, Schlunegger F, Rahn MK (2004) Climate-induced rebound and exhumation of the European Alps. Geology 32:709-712

Cerveny PF, Naeser ND, Zeitler PK, Naeser CW, Johnson NM (1988) History of uplift and relief of the Himalaya during the past 18 million years; evidence from sandstones of the Siwalik Group. *In*: New Perspectives in Basin Analysis. Kleinspehn KL, Paola C (eds) Springer-Verlag, New York, p 43-61

Copeland P, Harrison TM (1990) Episodic rapid uplift in the Himalaya revealed by $^{40}Ar/^{39}Ar$ analysis of detrital K-feldspar and muscovite, Bengal fan. Geology 18:354-357

Corrigan J (1991) Inversion of apatite fission track data for thermal history information. J Geophys Res 96: 10,347-10,360

Crowhurst PV, Green PF, Kamp PJJ (2002) Appraisal of (U+Th)/He apatite thermochronology as a thermal history tool for hydrocarbon exploration: An example from the Taranaki Basin, New Zealand. Am Assoc Petrol Geol Bull 86:1801-1819

Crowley KD (1993) Lenmodel: a forward model for calculating length distributions and fission-track ages in apatite. Computers and Geosciences 19:619-626

Crowley KD, Cameron M, Schaefer RL (1991) Experimental studies of annealing of etched fission tracks in fluorapatite. Geochim Cosmochim Acta 55:1449-1465

Deming D (1989) Application of bottom-hole temperature corrections in geothermal studies. Geothermics 18: 775-786

Dickinson WR (1993) Basin geodynamics. Basin Research 5:196-197

Donelick RA, O'Sullivan PB, Ketcham RA (2005) Apatite fission-track analysis. Rev Mineral Geochem 58: 49-94

Dow WG (1974) Application of oil-correlation and source-rock data to exploration in the Williston Basin. Am Assoc Petrol Geol Bull 80:1253-1262

Duddy IR (1994) The Otway Basin: thermal, structural, tectonic and hydrocarbon generation histories. *In*: NGMA/PESA Otway Basin Symposium, Extended Abstracts Record. Finalyson DM (ed) Australian Geological Survey Organisation, Canberra, p 35-42

Duddy IR, Green PF, Bray RJ, Hegarty KA (1994) Recognition of the thermal effects of fluid flow in sedimentary basins. *In*: Geofluids: Origin, Migration and Evolution of Fluids in Sedimentary Basins. Parnell J (ed) Geological Society Special Publication # 78, p 325-345

Ehlers TA (2005) Crustal thermal processes and the interpretation of thermochronometer data. Rev Mineral Geochem 58:315-350

Ehlers TA, Farley KA (2003) Apatite (U-Th)/He thermochronometry: methods and applications to problems in tectonic and surface processes. Earth Planet Sci Lett 206:1-14

Farley KA (2000) Helium diffusion from apatite: General behavior as illustrated by Durango fluorapatite. J Geophys Res 105:2909-2914

Farley KA (2002) (U-Th)/He dating: Techniques, calibrations, and applications. Rev Mineral Geochem 47: 819-843

Farley KA, Wolf RA, Silver LT (1996) The effects of long alpha-stopping distances on (U-Th)/He ages. Geochim Cosmochim Acta 60:4223-4229

Ferrero C, Gallagher K (2002) Stochastic thermal history modelling. 1. Constraining heat flow histories and their uncertainty. Mar Petrol Geol 19:633-648

Fitzgerald P, Gleadow AJW (1990) New approaches in fission track geochronology as a tectonic tool: Examples from the Transantarctic Mountains. Nucl Tracks Radiat Meas. 17:351-357

Funnell RH, Allis RG, Chapman DS, Armstrong PA (1996) Thermal regime of the Taranaki basin, New Zealand. J Geophys Res 101:25197-25215

Galbraith RF (1990) The radial plot: Graphical assessment of spread in ages. Nucl Tracks Radiat. Meas 17: 207-214

Galbraith RF, Green PF (1990) Estimating the component ages in a finite mixture. Nucl Tracks Radiat Meas 17:197-206

Galbraith RF, Laslett GM (1993) Statistical models for mixed fission track ages. Nucl Tracks Radiat Meas 21: 459-470

Gallagher K (1995) Evolving temperature histories from apatite fission-track data. Earth Planet Sci Lett 136: 421-435

Gallagher K, Sambridge M (1992) The resolution of past heat flow in sedimentary basins from non-linear inversion of geochemical data: the smoothest model approach with synthetic examples. Geophys J Int 109:78-95

Garver JI, Brandon MT, Roden-Tice M, Kamp PJJ (1999) Exhumation history of orogenic highlands determined by detrital fision-track thermochonology. *In*: Exhumation processes: Normal faulting, ductile flow and erosion. Ring U, Brandon MT, Lister GS, Willett SD (eds) Geological Society, London, p 283-304

Giles MR, Indrelid SL (1998) Divining burial and thermal histories from indicator data: application and limitations: An example from the Irish Sea and Cheshire Basins. *In*: Advances in Fission-Track Geochronology. Van den haute P, De Corte F (eds) Kluwer Academic Publishers, Dordrecht, p 115-150

Gleadow AJW, Belton DX, Kohn BP, Brown RW (2002) Fission track dating of phosphate minerals and the thermochronology of apatite. Rev Mineral Geochem 48:579-630

Gleadow AJW, Duddy IR (1981) A natural long-term annealing experiment for apatite. Nucl Tracks Radiat Meas 5:169-174

Gleadow AJW, Duddy IR, Lovering JF (1983) Fission track analysis; a new tool for the evaluation of thermal histories and hydrocarbon potential. APEA Journal 23:93-102

Gleadow AJW, Fitzgerald PG (1987) Uplift history and structure of the Transantarctic Mountains: New evidence from fission-track dating of basement apatites in the Dry Valleys area, southern Victoria Land. Earth Planet Sci Lett 82:1-14

Green PF, Duddy IR, Bray RJ (1995) Applications of thermal history reconstruction in inverted basins. *In*: Basin Inversion. Buchanan JG,Buchanan PG (eds) Geological Society of London, p 149-165

Green PF, Duddy IR, Gleadow AJW, Lovering JF (1989a) Apatite fission track analysis as a paleotemperature indicator for hydrocarbon exploration. *In*: Thermal History of Sedimentary Basins - Methods and Case Histories. Naeser ND,McCulloh T (eds) Springer-Verlag, New York, p 181-195

Green PF, Duddy IR, Gleadow AJW, Tingate PR (1985) Fission track annealing in apatite: track length measurements and the form of the Arrhenius plot. Nucl Tracks Radiat Meas 79:155-182

Green PF, Duddy IR, Laslett GM, Hegarty KA, Gleadow AJW, Lovering JF (1989b) Thermal annealing of fission tracks in apatite 4: quantitative modelling techniques and extension to geological timescales. Chem Geol (Isotope Geoscience Section) 79:155-182

Harrison TM, Be' K (1983) ^{40}Ar/^{39}Ar thermochronology of detrital microcline from the southern San Joaquin basin, California: an approach to determining the thermal evolution of sedimentary basins. Earth Planet Sci Lett 64:244-256

Harrison TM, Burke K (1989) ^{40}Ar/^{39}Ar thermochronology of sedimentary basins using detrital K-feldspars: Examplesfrom the San Joaquin Valley, California, Rio Grande Rift, New Mexico, and North Sea. *In*: Thermal History of Sedimentary Basins - Methods and Case Histories. Naeser ND, McCulloh TH (eds) Springer-Verlag, New York, p 141-155

Harrison TM, Zeitler PK (2005) Fundamentals of noble gas thermochronometry. Rev Mineral Geochem 58: 123-149

Hermanrud C (1993) Basin modelling techniques-an overview. *In*: Basin Modelling: Advances and Applications. Dore AG,Auguston JH,Hermanrud C,Stewart DJ,Sylta O (eds) Norwegian Petroleum Society (NPF), p 1-34

Hill KC, Hill KA, Cooper GT, O'Sullivan AJ, O'Sullivan PB, Richardson MJ (1995) Inversion around the Bass Basin, SE Australia. *In*: Basin Inversion. Buchanan JG, Buchanan PG (eds) Geological Society of London, p 525-547

Hodges KV, Ruhl KW, Wobus CW, Pringle MS (2005) ^{40}Ar/^{39}Ar thermochronology of detrital minerals. Rev Mineral Geochem 58:239-257

House MA, Farley KA, Kohn BP (1999) An empirical test of helium diffusion in apatite: borehole data from the Otway basin, Australia. Earth Planet Sci Lett 170:463-474

House MA, Kohn BP, Farley KA, Raza A (2002) Evaluating thermal history models for the Otway Basin, southeastern Australia, using (U+Th)/He and fission-track data from borehole apatites. Tectonophysics 349:277-295

Hu S, O'Sullivan PB, Raza A, Kohn BP (2001) Thermal history and tectonic subsidence of the Bohai Basin, northern China: a Cenozoic rifted and local pull-apart basin. Phys Earth Planet Intl 126:231-245

Ingersoll RV, Busby CJ (1995) Tectonics of sedimentary basins. *In*: Tectonics of sedimentary basins. Busby CJ, Ingersoll RV (eds) Blackwell Science, Oxford, p 1-51

Issler DR (1992) A new approach to shale compaction and stratigraphic restoration, Beaufort-Mackenzie basin and Mackenzie Corridor, northern Canada. Am Assoc Petrol Geol Bull 76:1170-1189

Issler DR (2004) AFTINV: An inverse multi-kinetic annealing model for apatite fission track thermal history reconstruction. 10th International Fission Track Dating and Thermochronology: 48

Issler DR, Willett SD, Beaumont C, Donelick RA, Grist AM (1999) Paleotemperature history of two transects across the Western Canada Sedimentary Basin: Constraints from apatite fission track analysis. Bull Can Petrol Geol 47:475-486

Kamp PJ, Green PF (1990) Thermal and tectonic history of selected Taranaki basin (New Zealand) wells assessed by apatite fission track analysis. Am Assoc Petrol Geol Bull 74:1401-1419

Kamp PJJ, Webster KS, Nathan S (1996) Thermal history analysis by integrated modelling of apatite fission track and vitrinite reflectance data: application to an inverted basin (Buller Coalfield, New Zealand). Basin Res 8:383-402

Ketcham RA (2005) Forward and inverse modeling of low-temperature thermochronometry data. Rev Mineral Geochem 58:275-314

Ketcham RA, Donelick RA, Carlson WD (1999) Variability of apatite fission-track annealing kinetics: III. Extrapolation to geological time scales. Am Mineral 84:1235-1255

Ketcham RA, Donelick RA, Donelick MB (2000) AFTSolve: A program for multi-kinematic modeling of apatite fission-track data. Geol Mat Res 2:1-32

King PR, Thrasher GP (1996) Cretaceous-Cenozoic geology and petroleum systems of the Taranaki Basin, New Zealand. Institute of Geological and Nuclear Sciences Limited, Lower Hutt, 6 enclosures

Kohn BP, Feinstein S, Foster DA, Steckler MS, Eyal M (1997) Thermal history of the eastern Gulf of Suez, II. Reconstruction from apatite fission track and ^{40}Ar/^{39}Ar K-feldspar measurements. Tectonophysics 283: 219-239

Laslett GM, Gleadow AJW, Duddy IR (1987) Thermal annealing of fission tracks in apatite 2: a quantitative analysis. Chem Geol (Isotope Geoscience Section) 65:1-13

Lerche I (1993) Theoretical aspects of problems in basin modelling. *In*: Basin Modelling: Advances and Applications. Dore AG, Auguston JH, Hermanrud C, Stewart DJ, Sylta O (eds) Norwegian Petroleum Society (NPF), p 35-65

Lim HS, Lee Y, Min KD (2003) Thermal history of the Cretaceous Sindong Group, Gyeongsang Basin, Korea based on fission track analysis. Basin Res 15:139-152

Lippolt HJ, Leitz M, Wernicke RS, Hagedorn B (1994) (U+Th)/He dating of apatite: experience with samples from different geochemical environments. Chem Geol 112:179-191

Lopatin NV (1971) Temperature and geologic time as factors in coalification. Izv Akad Nauk SSSR 3:95-106

Lorencak M, Kohn BP, Osadetz KG, Gleadow AJW (2004) Combined apatite fission track and (U-Th)/He thermochronometry in a slowly cooled terrane: results from a 3440-m-deep drill hole in the southern Canadian Shield. Earth Planet Sci Lett 227:87-104

Lovera OM, Grove M, Harrison TM, Mahon KI (1997) Systematic analysis of K-Feldspar 40Ar/39Ar step-heating experiments: I. Significance of activation energy determinations. Geochim Cosmochim Acta 61: 3171-3192

Magara K (1976) Thickness of removed sedimentary rocks, Paleopore pressure and paleotemperatures, southwestern part of western Canada Basin. Am Assoc Petrol Geol Bull 60:554-565

Mahon KI, Harrison TM, Grove M (1998) The thermal and cementation histories of a sandstone petroleum reservoir, Elk Hills, California. Chem Geol 152:227-256

Marshallsea SJ, Green PF, Webb J (2000) Thermal history of the Hodgkinson Province and Laura Basin, Queensland: Mutiple cooling episodes identified from apatite fission track analysis and vitrinite reflectance data. Austral J Earth Sci 47:779-797

McDougall I, Harrison TM (1999) Geochronology and Thermochronology by the $^{40}Ar/^{39}Ar$ Method. Oxford University Press, Oxford

McKenzie D (1978) Some remarks on the development of sedimentary basins. Earth Planet Sci Lett 40:25-32

Naeser CW (1979) Thermal history of sedimentary basins in fission track dating of subsurface rocks. SEPM Special Publication 26:109-112

Naeser CW (1993) Apatite fission-track analysis in sedimentary basins-a critical appraisal. *In*: Basin Modeling: Advances and applications. Dore AG, Auguston JH, Hermanrud C, Stewart DJ, Sylta O (eds) Norwegian Petroleum Society, p 147-160

Naeser ND, Naeser CW, McCulloh TH (1989) The application of fission-track dating to depositional and thermal history of rocks in sedimentary basins. *In*: Thermal History of Sedimentary Basins - Methods and Case Histories. Naeser ND, McCulloh TH (eds) Springer-Verlag, New York, p 157-180

Naeser ND, Naeser CW, McCulloh TH (1990) Thermal history of rocks in southern San Joaquin Valley, California: Evidence from fission-track analysis. Am Assoc Petrol Geol Bull 74:13-29

Najman YMR, Pringle MS, Johnson MRW, Robertson AHF, Wijbrans JR (1997) Laser $^{40}Ar/^{39}Ar$ dating of single detrital muscovite grains from early foreland-basin sedimentary deposits in India: Implications for early Himalayan evolution. Geology 25:535-538

Nielsen SB (1996) Sensitivity analysis in thermal and maturity modelling. Mar Petrol Geol 13:415-425

Nielsen SB, Balling N (1990) Modelling subsidence, heat flow, and hydrocarbon generation in extensional basins. First Break 8:23-31

Osadetz KG, Kohn BP, Feinstein PB, O'Sullivan PB (2002) Thermal history of Canadian Williston basin from apatite fission-track thermochronology-implications for petroleum systems and geodynamic history. Tectonophysics 349:221-249

O'Sullivan PB (1999) Thermochronology, denudation and variations in paleosurface temperature: a case study from the North Slope foreland basin, Alaska. Basin Res 11:191-204

O'Sullivan PB, Brown RW (1998) Effects of surface cooling on apatite fission track data: Evidence or Miocene climatic change, North Slope, Alaska. *In*: Advances in fission track geochronology. Van den haute P, De Corte F (eds) Kluwer Academic Publishers, Dordrecht, p 255-267

O'Sullivan PB, Parrish RR (1995) The importance of apatite composition and single-grain ages when interpreting fission track data from plutonic rocks: A case study from the Coast Ranges, British Columbia. Earth Planet Sci Lett 132:213-224

O'Sullivan PB, Wallace WK (2002) Out-of-sequence, basement-involved structures in the Sadlerochit Mountains region of the Arctic National Wildlife Refuge, Alaska: Evidence and implications from fission-track thermochronology. Geol Soc Am Bull 114:1356-1378

Pagell M, Braun JJ, Disnar JR, Martinez L, Renac C, Vasseur G (1997) Thermal history constraints from studies of organic matter, clay minerals, fluid inclusions and apatite fission tracks at the Ardeche paleo-margin (BAI Drill Hole, CPF Program). J Sed Res 67:235-245

Parnell J, Carey PF, Green PF, Duncan W (1999) Hydrocarbon migration history, West of Shetland: Integrated fluid inclusion and fission track studies. *In*: Petroleum Geology of Northwest Europe. Fleet JJ, Boldy SAR (eds) Proc 5th Conf. Geological Society of London, p 613-625

Poelchau HS, Baker DR, Hantschel T, Horsfield B, Wygrala B (1997) Basin simulation and the design of the conceptual basin model. *In*: Petroleum and Basin Evolution. Welte DH, Horsfield B, Baker DR (eds) Springer, p 5-70

Rahl JM, Reiners PW, Campbell IH, Nicolescu S, Allen CM (2003) Combined single-grain (U-Th)/He and U/Pb dating of detrital zircons from the Navajo Sandstone, Utah. Geology 31:761-764

Ravenhurst CE, Willett SD, Donelick RA, Beaumont C (1994) Apatite fission track thermochronometry from central Alberta: Implications for the thermal history of the Western Canada Sedimentary Basin. J Geophys Res 99:20023-20041

Reiners PW (2005) Zircon (U-Th)/He thermochronometry. Rev Mineral Geochem 58:151-179

Reiners PW, Farley KA (2001) Influence of crystal size on apatite (U-Th)/He thermochronology: an example from the Bighorn Mountains, Wyoming. Earth Planet Sci Lett 188:413-420

Reiners PW, Farley KA, Hickes HJ (2002) He diffusion and (U-Th)/He thermochronology of zircon: Initial results from Fish Canyon Tuff (Colorado) and Gold Butte (Nevada). Tectonophysics 349:247-308

Rorhman M, Andreissen P, van der Beck P (1996) The relationship between basin and margin thermal evolution assessed by FT thermochronology: an application to offshore southern Norway. Basin Res 8:45-63

Ruiz GMH, Seward D, Winkler W (2004) Detrital thermochronology-a new perspective on hinterland tectonics, an example from the Andean Amazon Basin, Ecuador. Basin Res 16:413-430

Sambridge MS, Compston W (1994) Mixture modelling of multi-component data sets with application to ion probe zircon ages. Earth Planet Sci Let 128:373-390

Sclater JG, Christie PAF (1980) Continental stretching: An explanation of the post-mid-cretaceous subsidence of the central North Sea Basin. J Geophys Res 85:3711-3739

Sobel ER, Dumitru TA (1997) Thrusting and exhumation around the margins of the western Tarim basin during the India-Asia collision. J Geophys Res 102:5043-5063

Spiegel C, Kuhlemann J, Dunkl I, Frisch W, von Eynatten H, Kadosa B (2000) Erosion history of the Central Alps: evidence from zircon fission track data of the foreland basin sediments. Terra Nova 12:163-170

Spiegel C, Siebel W, Kuhlemann J, Frisch W (2004) Toward a more comprehensive provenance analysis: A multi-method approach and its implications for the evolution of the Central Alps. *In*: Detrital Thermochronology: Provenance Analysis, Exhumation, and Landscape Evolution of Mountain Belts. Bernet M, Spiegel C (eds) Geological Society of America, p 37-50

Stockli DF, Farley KA, Dumitru TA (2000) Calibration of the apatite (U-Th)/He thermochronometer on an exhumed fault block, White Mountains, California. Geology 28:983-986

Tagami T (2005) Zircon fission-track thermochronology and applications to fault studies. Rev Mineral Geochem 58:95-122

Tagami T, O'Sullivan PB (2005) Fundamentals of fission-track thermochronology. Rev Mineral Geochem 58: 19-47

Tissot BP, Welte DH (1978) Petroleum Formation and Occurrence: A New Approach to Oil and Gas Exploration. Springer-Verlag, Berlin

Ventura B, Pini GA, Zuffa GG (2001) Thermal history and exhumation of the Northern Apennines (Italy): evidence from combined apatite fission track and vitrinite reflectance data from foreland basin sediments. Basin Res 13:435-448

Weir LA, Furlong KP (1987) Thermal regimes of small basins: Effects of intrabasinal conductive and advective heat transport. *In*: Sedimentary Basins and Basin Forming Mechanisms. Beaumont C, Tankard AJ (eds) Can Soc Petrol Geol p 351-362

Weissel JK, Hayes DE (1977) Evolution of the Tasman Sea reappraised. Earth Planet. Sci Lett 36:77-84

White NM, Pringle MS, Garzanti E, Bickle M, Najman Y, Chapman H, Friend P (2002) Constraints on the exhumation and erosion of the High Himalayan Slab, NW India, from foreland basin deposits. Earth Planet Sci Lett 195:29-44

Willett S, Brandon MT (2002) On steady states in mountain belts. Geology 30:175-178

Willett SD (1988) Spatial variation of temperature and thermal history of the Uinta Basin Type thesis, Univ. of Utah

Willett SD (1992) Modelling thermal annealing of fission tracks in apatite. *In*: Short Course on Low Temperature Thermochronology. Zentilli M,Reynolds PH (eds) p 42-74

Willett SD (1997) Inverse modeling of annealing of fission tracks in apatite 1:A controlled random search method. Am J Sci 297:939-969

Wolf RA, Farley KA, Kass DM (1998) Modeling of the temperature sensitivity of the apatite (U-Th_/He thermochronometer. Chem Geol 148:105-114

Wolf RA, Farley KA, Silver LT (1996) Helium diffusion and low-temperature thermochronometry of apatite. Geochim Cosmochim Acta 60:4231-4240

Zeitler PK, Herczeg AL, McDougall I, Honda M (1987) U-Th-He dating of apatite: A potential thermochronometer. Geochim Cosmochim Acta 51:2865-2868

Zeitler PK, Johnson NM, Briggs ND, Naeser CW (1986) Uplift history of the NW Himalaya as recorded by fission-track ages of detrital Siwalik zircons. *In*: Proceedings of the Symposium on Mesozoic and Cenozoic Geology. Jiqing H (ed) Geological Publishing House, Beijing, p 481-494